

Probing the quark-gluon plasma with a new Fermionic correlator

R. V. Gavai* and Sourendu Gupta†

*Department of Theoretical Physics, Tata Institute of Fundamental Research,
Homi Bhabha Road, Mumbai 400005, India.*

Abstract

We present the first measurement of a new correlation function of Fermion bilinears in finite temperature QCD with and without dynamical quarks in a quantum number channel in which non-trivial correlations are known to be present for purely gluonic operators. We find that the Fermion correlator vanishes for $T \geq 3T_c/2$, in agreement with the expectation for weakly interacting quarks in a quark-gluon plasma.

11.15.Ha, 12.38.Mh

Typeset using REVTeX

*Electronic mail: gavai@tifr.res.in

†Electronic mail: sgupta@tifr.res.in

The Relativistic Heavy Ion Collider (RHIC) in BNL, New York and the Large Hadron Collider (LHC) in CERN, Geneva may yield a new state of matter, called Quark-Gluon Plasma (QGP), which could have existed in our universe a few microseconds after the Big Bang. It is a theoretically challenging task to deduce from first principles as many properties of the plasma as possible. Such a program may help in devising clear and unique signals of QGP.

Lattice simulations of Quantum Chromo Dynamics (QCD) have provided a robust approach based on first principles towards this end. Such simulations of field theories in equilibrium at finite temperature (T) use a discretisation of the Euclidean formulation for partition functions—

$$Z(\beta) = \int \mathcal{D}\phi \exp \left[- \int_0^{1/T} dt \int d^3x \mathcal{L}(\phi) \right], \quad (1)$$

where ϕ is a generic field, \mathcal{L} the Lagrangian density, and the Euclidean “time” runs from 0 to $1/T$. The path integral is over field configurations which are periodic (anti-periodic) in Euclidean time for the Bosonic gluon (Fermionic quark) fields. Due to a lack of symmetry between the space and Euclidean time directions in Eq. (1), this problem has only a subgroup of the full 4-dimensional rotational symmetry of the $T = 0$ Euclidean theory. For the lattice discretised problem each of these groups is further reduced to a discrete subgroup.

For the lattice problem it is more useful to write the partition function of Eq. (1) as the trace of the transfer matrix in one of the spatial directions. Correlation functions along that direction can then be classified by the irreducible representations (irreps) of the symmetry group of the transfer matrix. At $T = 0$, the symmetry group of the transfer matrix for QCD using the staggered Fermions for quarks has been studied extensively, and the representations of corresponding Fermion bilinear correlation functions are well known [1]. The symmetries and representations of screening correlation functions at finite temperature have been worked out recently [2].

The main point of this last analysis is that the symmetry group of the $T > 0$ transfer matrix is smaller than that of the $T = 0$ transfer matrix. As a result, the $T = 0$ irreps reduce further at finite temperature. All correlation functions block diagonalise under the isometry group of the spatial slice of the thermal lattice, the dihedral group D_4^h . As an example, a correlation function in, say, the z -direction of any vector or pseudo-vector operator, (V_x, V_y, V_t) , in the $T = 0$ theory breaks up into two scalar (A_1^+) irreps of D_4^h , the components V_t and $V_x + V_y$, and a B_1^+ irrep $V_x - V_y$. This happens for gluonic Wilson-loop operators such as plaquettes, and also for the quark bilinears operators shown in Table I.

In quenched QCD, i.e., without dynamical quarks, it is known that the finite-temperature scalar (A_1^+) channel probed by gluonic operators reveals a non-trivial screening mass related to the Debye screening mass, m_D , in the theory. Non-trivial screening has been observed through gauge-invariant gluonic correlation functions [3] in all the other quantum number channels (labelled by the irreps of D_4^h) as well. For $T \geq 2T_c$ the degeneracies of these screening masses show dimensional reduction. The screening mass in the B_1^+ channel is substantially larger than that in the A_1^+ channel.

Screening masses obtained from correlation functions built out of staggered Fermion field operators have also been extensively studied in the past [4–6]. The correlators which have been measured in the past are the A_1^+ from the scalar (S) and pseudo-scalar (PS) channels,

and A_1^+ combinations of the vector (V) and pseudo-vector (PV) channels. The two A_1^+ correlators descending from S and PS see a lower screening mass (μ) than those descending from the V and PV. The latter are consistent with the expectation from free Fermion field theory—

$$\mu a = 2 \sinh^{-1} \left(\sqrt{(ma)^2 + \sin^2 \left(\frac{\pi}{N_t} \right)} \right), \quad (2)$$

where a is the lattice spacing, m the quark mass, and N_t is the number of lattice sites in the Euclidean time direction ($T = 1/N_t a$). Even some other measurements, such as those of “wavefunctions”, which seemed to indicate a more complicated picture [7], can be understood in terms of weakly interacting quarks [8]. Here we re-examine the screening masses with the complete decomposition of operators into irreps of the finite temperature invariance group. In particular, we report in this letter the results of the first measurement of the B_1^+ correlation function constructed from local Fermion bilinears (Table I) and compare our results with those obtained with gluonic operators.

We have simulated QCD with four light degenerate flavors of quarks at temperatures above the phase transition temperature, T_c , on lattices of size $4 \times 10^2 \times 16$, using the Hybrid Monte Carlo (HMC) algorithm [9]. The longest direction, N_z , was chosen to be four times the Euclidean time direction, N_t , so that correlations could be followed to a distance of $2/T$. One simulation was performed at $T = 3T_c/2$ with the coupling $\beta = 5.1$ and the quark mass $m = 0.015/a$ where a is the lattice spacing. The second simulation was made at $T = 2T_c$ with $\beta = 5.15$ and $m = 0.01/a$. With our choice of $N_t = 4$, $a = 1/4T$. The temperature identifications are made using previous measurements of the critical coupling on lattices with larger values of N_t [10]. Companion runs were made in quenched QCD on lattices of the same size at couplings corresponding to $3T_c/2$ and $2T_c$ for the quenched theory using a Cabbibo-Marinari pseudo-heat-bath algorithm [11].

We thermalised the HMC simulation at $3T_c/2$ with two different runs— one starting from an ordered gauge configuration, and the other from a pure gauge configuration thermalised at $2T_c$. Agreement in measurements of all thermodynamic quantities was used to decide on thermalisation. The plaquette average turned out to be the most stringent test, since it is the least noisy. At $2T_c$ thermalisation was tested by checking that a run starting from an ordered gauge configuration gave the same thermodynamics as one starting from a thermal $3T_c/2$ configuration.

Once thermalisation was achieved, two runs were made at each temperature— one with a trajectory length of one molecular dynamics (MD) time unit, and another with a trajectory length half as long. At $3T_c/2$ statistics was collected from 875 such configurations generated using the long trajectory, and 285 with the short trajectory. Previous studies have shown that the physics is much simpler at $2T_c$. We did smaller runs at this temperature— collecting statistics of 445 configurations with the short trajectory length and 100 with the long trajectories.

The question of autocorrelations is important whenever statistical inferences are to be made. It was found that autocorrelations of local operators, such as plaquettes, were the same with the two different trajectory lengths mentioned above. However, with any simulation algorithm that undergoes critical slowing down, short distance operators are decorrelated faster than those which are dominated by large distance scales. Thus, the effective

number of measurements of short distance operators is not the same as that for extended operators. This is most problematic for correlation function measurements, where the correlator at different distances may have entirely different autocorrelations. These are usually difficult to measure directly and a different approach to the problem seems necessary.

If the errors in Fermion bilinear correlation functions, $\Delta C(z)$, are evaluated with the assumption that there are no autocorrelations, then they depend systematically on the separation z . We found that for sufficiently large statistics, $\Delta C(z)$ falls exponentially with z and its logarithmic slope is almost independent of statistics. Hence it is possible to quote a single number as a figure of merit for decorrelation—

$$D = \frac{\Delta C(N_z/2)}{\Delta C(0)}. \quad (3)$$

D is usually larger than unity, and depends on the specifics of the simulation algorithm and its tuning. Since smaller values of D are preferable, tuning the algorithm should be done to minimise this.

The values of D obtained depended on the channel being studied: the largest values of D were found in the A_1^+ irreps coming from the V or the PV, and the smallest in the B_1^+ irreps. In each channel, we found only a weak dependence of D on the number of measurements—indicating that it is a direct measure of the efficiency of the algorithm.

We found that the long trajectories (1 MD time unit) give about half the value of D as obtained with the shorter trajectory. Since it takes twice as long to run the longer trajectory, the computational effort

$$E = D \times (\text{CPU time}) \quad (4)$$

involved in getting equal statistical errors is the same for these two trajectory lengths. However, the analysis of correlated errors in screening mass measurements is simplified with the longer trajectories. In test runs with trajectories 2.5 MD time units long, we found no further decrease in D , and hence an increase in E . Such a dependence of E on trajectory length has been found to be characteristic of the HMC simulation algorithm [12]. In the dynamical QCD simulations, we found D to lie in the range 250 to 1000. The quenched simulations were significantly easier to decorrelate—the value of D was lower by a factor of roughly 40 compared to the full theory simulations. This information on autocorrelations has been incorporated in all our statistical analyses.

In Table II, we report our measurements of screening masses for the known A_1^+ correlators. Our results for the quenched computations are seen to be in very good agreement with previous measurements [6]. There is also a remarkable agreement between the A_1^+ screening masses obtained from the quenched and the dynamical Fermions simulations at both temperatures. The four A_1^+ irreps coming from the V and PV channels gave degenerate screening masses which agree extremely well with the free field theory estimate in Eq. (2). The A_1^+ correlators in the S and PS channels gave smaller screening masses, which increase marginally with T .

Hadron mass measurements in 4-flavor QCD at quark mass, $ma = 0.01$ and $\beta = 5.15$, corresponding to our runs at $2T_c$, have been performed before [13]. A comparison with these $T = 0$ measurements, listed in the last column of Table II, shows that our finite temperature screening masses are completely different—

$$\frac{\mu(T)}{m(T=0)} \approx \begin{cases} 3 & (A_1^+ \text{ from PS}), \\ 2 & (A_1^+ \text{ from V}). \end{cases} \quad (5)$$

In contrast, earlier measurements for $N_t = 8$ lattices yielded $\mu/m \approx 1$ for the A_1^+ screening mass in the vector channel V [5]. This made it difficult to argue for a thermal effect, although μ agreed with Eq. (2) even in that case. The present measurement resolves this problem.

Some of our measurements were also made with fuzzed links. Unlike recent studies [14], where these “fat links” were used as part of an improved action program, we have used fuzzing only for signal improvement. We defined the fat links [3] at level $l + 1$ of fuzzing recursively by the definition—

$$U_\mu^{l+1}(x) = \left[\sum_{\nu \neq \mu, \hat{z}} U_\nu^l(x) U_\mu^l(x + \nu) (U_\nu^l(x + \mu))^\dagger \right]_{SU(3)}, \quad (6)$$

where $l = 0$ denotes the links obtained directly from simulation. The links at each level were used to determine the Fermion propagators. The higher fuzzing levels gave A_1^+ masses consistent with each other, and all of them were consistent with Eq. (2).

Our main new result is the first measurement of the correlation function in the B_1^+ channels. Correlators in this irrep obtained with PV and V are identical up to a sign, configuration by configuration. Hence we restrict our attention only to the B_1^+ coming from the V. We found that the B_1^+ correlation functions vanish to the best of the measurement precision (see Figure 1). The correct statistical procedure is to quote the χ^2 value for the fit of the data by a correlation function which is identically zero. We found

$$\chi^2/\text{DOF} = \begin{cases} 7/15 & (3T_c/2, \text{ dynamical}), \\ 11/15 & (2T_c, \text{ dynamical}). \end{cases} \quad (7)$$

The quenched runs gave very similar results—

$$\chi^2/\text{DOF} = \begin{cases} 7/15 & (3T_c/2, \text{ quenched}), \\ 5/15 & (2T_c, \text{ quenched}). \end{cases} \quad (8)$$

The numbers in Eq. (7) have been obtained with the statistics collected in the longer of the two runs made at each temperature. The HMC simulations with smaller statistics also gave very similar results at both these temperatures.

One possible explanation for these remarkable results is that the theory at finite temperature has a dynamical generation of the symmetry of the $T = 0$ system. As a result, there is a symmetry between the x and y polarisations of a V and PV, and hence the B_1^+ correlator vanishes, being the difference of the two. Since the screening mass measurements have already shown a large difference between $T = 0$ and finite temperature theories, as discussed above, we do not expect this argument to be correct. Nevertheless, a more direct test of this explanation is also possible.

We test for the equivalence between the x and y components at $T > 0$ of a gluonic operator which is either a vector or a pseudo-vector at $T = 0$. The plaquette operators, restricted to a z -slice are an example. The combinations P_{xy} and $P_{tx} + P_{ty}$ transform as the A_1^+ component of the PV, and $P_{tx} - P_{ty}$ as the B_1^+ [3]. The plaquette averages do show the x - y symmetry, since the difference of the averages vanishes within errors —

$$\langle P_{tx} - P_{ty} \rangle = \begin{cases} (-0.6 \pm 1.8) \times 10^{-4} & (3T_c/2, \text{ quenched}), \\ (5.5 \pm 3.8) \times 10^{-5} & (2T_c, \text{ quenched}). \end{cases} \quad (9)$$

However, its correlation function does not. The same configurations used in the Fermionic correlator measurements lead to gluonic B_1^+ correlations which are clearly non-zero. The correlation function of $P_{tx} - P_{ty}$ is exhibited in Figure 2 for the quenched QCD simulations. Since the corresponding screening mass is large [3], the correlation function is somewhat noisy at large distances but it is clearly very different from zero at small distances. The test of a vanishing value of this correlation function gives $\chi^2/\text{DOF} \approx 800$. Thus the gauge configurations underlying our measurements have a strong configuration-to-configuration asymmetry between the x and y directions, allowing the gluonic B_1^+ correlators to survive, although the corresponding operator average is zero.

Having ruled out an exact x - y symmetry, we are left with the conclusion that the Fermionic correlators behave as if they see a weakly interacting quark-gluon plasma. The Fermionic B_1^+ correlators studied here are identically zero in free field theory. Consequently, they give direct evidence for the weakly interacting picture by acting like an order parameter which is nonzero for interacting Fermions. Earlier, one had to rely on the numerical agreement of the screening masses extracted from the exponential fall-off of the A_1^+ -correlators with free field values of Eq. (2) to reach this conclusion. Thus the B_1^+ correlator is a qualitatively better indicator of the non-interacting nature of the quarks in the quark-gluon plasma.

The drawback of this non-interacting picture is well-known— the A_1^+ irreps coming from the S and PS channels are not degenerate with those coming from the V and PV channels. A plausible argument to understand this phenomenon is to note that the A_1^+ correlator coming from the S channel mixes with the glue sector of the theory. As a result, the screening mass in this channel will be contaminated by those in the gluonic A_1^+ sector, of which the lowest is the Debye screening mass, m_D . In quenched simulations at $3T_c/2$, $m_D/T = 2.8 \pm 0.2$ [3]. Since the screening mass for the S channel lies in between m_D and the V channel mass, as seen in Table II, it is consistent with such a conjecture.

We employed staggered Fermions for this investigation. It would be interesting to confirm these results for the Wilson Fermions as well. The symmetries of the lattice are, of course, independent of the type of Fermions employed and the group theoretic arguments apply with small modifications. In particular, the break-up of the zero temperature spectrum under the D_4^h group proceeds without change. The actual operators realising the irreps listed in Table I will certainly change.

To summarize, we have used a new Fermionic correlator to demonstrate that the quarks in the quark-gluon plasma are weakly interacting already at temperatures as low as $3T_c/2$. The particular correlator we used is a much better probe of Fermion interaction strength than those used earlier and acts like an order parameter.

REFERENCES

- [1] H. Kluberg-Stern *et al.*, *Nucl. Phys.*, B 220 (1983) 447; M. F. L. Golterman and J. Smit, *Nucl. Phys.*, B 255 (1985) 328; M. F. L. Golterman, *Nucl. Phys.*, B 273 (1986) 663.
- [2] S. Gupta, e-print hep-lat/9903019.
- [3] B. Grossmann *et al.*, *Nucl. Phys.*, B 417 (1994) 289; S. Datta and Sourendu Gupta, *Nucl. Phys.*, B 534 (1998) 392.
- [4] C. DeTar and J. Kogut, *Phys. Rev. Lett.*, 59 (1987) 399; *Phys. Rev.*, D 36 (1987) 2828; S. Gottlieb, *et al.*, *Phys. Rev. Lett.*, 59 (1987) 1881; A. Gocksch, P. Rossi and U. M. Heller, *Phys. Lett.*, B 205 (1988) 334; G. Boyd, S. Gupta and F. Karsch, *Nucl. Phys.*, B 385 (1992) 481. T. Hashimoto, T. Nakamura and I. O. Stamatescu, *Nucl. Phys.*, B 400 (1993) 267; Ph. de Forcrand *et al.*, e-print hep-lat/9901017.
- [5] K. Born, *et al.*, (The MT_c collaboration), *Phys. Rev. Lett.*, 67 (1991) 302.
- [6] S. Gupta, *Phys. Lett.*, B 288 (1992) 171.
- [7] C. Bernard, *et al.*, *Phys. Rev. Lett.*, 68 (1992) 2125.
- [8] T. H. Hansson and I. Zahed, *Nucl. Phys.*, B 374 (1992) 277; V. Koch *et al.*, D 46 (1992) 3169.
- [9] S. Duane, A. D. Kennedy, B. J. Pendleton and D. Roweth, *Phys. Lett.*, B 195 (1987) 216.
- [10] F. R. Brown, *et al.*, *Phys. Lett.*, B 221 (1990) 181; R. V. Gavai, *et al.*, (The MT_c collaboration), *Phys. Lett.*, B 241 (1990) 567.
- [11] N. Cabibbo and E. Marinari, *Phys. Lett.*, 119 B (1982) 387.
- [12] S. Gupta, *Nucl. Phys.*, B 370 (1992) 741.
- [13] R. Altmeyer *et al.*, (The MT_c collaboration), *Nucl. Phys.*, B 389 (1993) 445.
- [14] T. DeGrand, A. Hasenfratz and T. G. Kovács, e-print hep-lat/9807002; T. DeGrand, e-print hep-lat/9903006; K. Orginos, D. Toussaint and R. L. Sugar, e-print hep-lat 9903032.

FIGURES

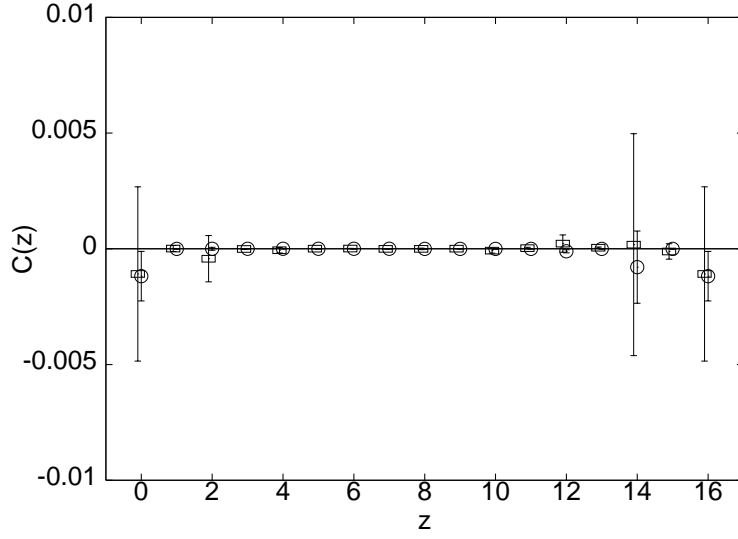


FIG. 1. The B_1^+ correlation function obtained from the V channel operators. Boxes denote data for dynamical QCD simulations for $3T_c/2$ and circles for $2T_c$.

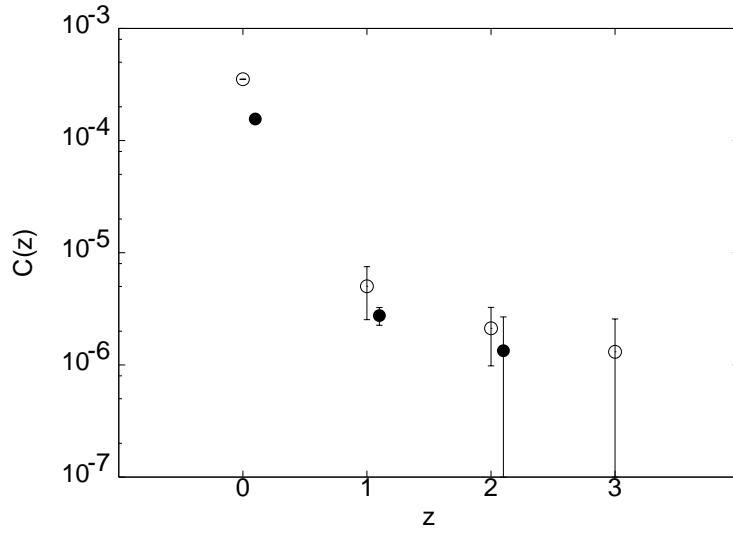


FIG. 2. The B_1^+ correlation function obtained from the plaquette operators. Filled circles denote data for $3T_c/2$ and open for $2T_c$.

TABLES

Name	D_4^h	Operator
PS	A_1^+	$\sum_x \bar{\chi}(x)\chi(x)$
S	A_1^+	$\sum_x \eta_4(x)\zeta_4(x)\bar{\chi}(x)\chi(x)$
V	A_1^+	$\sum_x \epsilon(x)\eta_3(x)\zeta_3(x)\bar{\chi}(x)\chi(x)$
	A_1^+	$\sum_x \epsilon(x)[\eta_1(x)\zeta_1(x) + \eta_2(x)\zeta_2(x)]\bar{\chi}(x)\chi(x)$
	B_1^+	$\sum_x \epsilon(x)[\eta_1(x)\zeta_1(x) - \eta_2(x)\zeta_2(x)]\bar{\chi}(x)\chi(x)$
PV	A_1^+	$\sum_x \epsilon(x)\eta_4(x)\zeta_4(x)\eta_3(x)\zeta_3(x)\bar{\chi}(x)\chi(x)$
	A_1^+	$\sum_x \epsilon(x)\eta_4(x)\zeta_4(x)[\eta_1(x)\zeta_1(x) + \eta_2(x)\zeta_2(x)]\bar{\chi}(x)\chi(x)$
	B_1^+	$\sum_x \epsilon(x)\eta_4(x)\zeta_4(x)[\eta_1(x)\zeta_1(x) - \eta_2(x)\zeta_2(x)]\bar{\chi}(x)\chi(x)$

TABLE I. Representations of local staggered Fermion bilinears. Here $\epsilon(x) = (-1)^{x_1+x_2+x_3+x_4}$, $\eta_i(x) = \prod_{k<i}(-1)^{x_k}$ and $\zeta_i(x) = \prod_{k>i}(-1)^{x_k}$. The sum over x runs over all sites on a z -slice. The interpretation in terms of mesons at $T = 0$ is clear from the names.

Channel	$3T_c/2$ D	$3T_c/2$ Q	$2T_c$ D	$2T_c$ Q	$T = 0$
S A_1^+	0.91 ± 0.03	1.08 ± 0.01	1.07 ± 0.04	1.14 ± 0.02	0.60 ± 0.05
PS A_1^+	0.91 ± 0.03	1.05 ± 0.01	1.07 ± 0.04	1.13 ± 0.01	0.303 ± 0.002
V A_1^+	1.39 ± 0.07	1.33 ± 0.03	1.35 ± 0.06	1.36 ± 0.02	0.71 ± 0.06
PV A_1^+	1.39 ± 0.07	1.37 ± 0.05	1.35 ± 0.06	1.38 ± 0.04	1.4 ± 0.1

TABLE II. Screening masses in units of the lattice cutoff, $1/a = T/4$, from quenched (Q) and dynamical quark simulations (D). The $T = 0$ masses quoted here were measured [13] with the same lattice spacing and quark mass as the runs at $2T_c$ (D).